ICANS-XIV
14th Meeting of the International Collaboration on
Advanced Neutron Sources
June 14-19, 1998
Argonne National Laboratory, 9700 S. Cass Avenue, Argonne, IL 60439, USA

Measurement and Analysis of Reaction Rate Distributions in A Lead Assembly Containing Tungsten Target with 500 MeV Proton Bombardment

H.Takada, S.Meigo, T.Sasa and K.Tsujimoto

Center for Neutron Science
Japan Atomic Energy Research Institute
Tokai-mura, Naka-gun, Ibaraki-ken, 319-1195, JAPAN

Abstract

In order to study the production and transport of spallation neutrons in a thick medium for the 500 MeV proton bombardment, an integral experiment was carried out using a lead assembly in which a tungsten target is placed in the center. The reaction rate distributions were measured with various activation detectors by the γ-ray spectrometry in the experiment. The analytical study was also performed using the NMTC/JAERI-MCNP4A code system with the nuclide production cross section values combining JENDL Dosimetry File and the ALICE-F calculation. The calculations using this code system reproduce the measured reaction rates with an accuracy of 20 to 30%.

1. Introduction

The Monte Carlo simulation code system NMTC/JAERI (1) combining MCNP4A (2) has been employed for the analysis of spallation experiments in JAERI. The code system is considered as a tool for neutronics design of the facilities proposed for the neutron science project (3). Experimental benchmark is required to validate the code system for estimating the source term as accurate as possible in the neutronic design study. The MCNP4A code itself and associated evaluated nuclear data below 20 MeV have been validated very well through the activities related to the fusion neutronics. Thus, the major interest is focused on the validation of the NMTC/JAERI code which simulates the production and transport of spallation neutrons in a thick medium.

As experimental data available for benchmark are very limited, we have started the thick target experiments (4,5) together with a thin target one (6). In the previous work (5), the transport of spallation neutrons in a lead assembly were studied using the activation detectors for 500 MeV proton bombardment at the beam dump room of the booster synchrotron utilization facility of High Energy Accelerator Research Organization (KEK). In this work, the reaction rate distribution of the activation detectors were measured in the lead assembly in which tungsten target was placed in the center aiming at studying the neutron production and transport dependent upon the target material. Tungsten was chosen because it was one of promising materials for an intense spallation target driven by a proton accelerator with power of MW. For

Keywords: lead assembly installing tungsten target, 500 MeV proton, activation detector, NMTC/JAERI

convenience, the lead assembly containing the tungsten target is denoted as 'tungsten/lead assembly' in this paper.

2. Experimental Procedure

The experimental procedure was essentially the same as for the previous work (5). Figure 1 shows the cross sectional view of the tungsten/lead assembly. The size of the assembly was 60 cm in outer diameter and 100 cm in length. A 16 cm outer diameter and 30 cm long tungsten alloy target with weight fractions of 97 % W, 1% Ni and 2% Cu was embedded in the lead assembly. The tungsten target and the lead assembly was covered with 2.5 mm thick stainless steel (SS) plates, respectively. The protons were transported through a beam entrance hole of 10 cm in diameter and were injected perpendicular to the tungsten target surface.

The high purity metal pellets of Al, Ni, Au and Nb were used as the activation detectors. The diameter of pellets was 8 mm. The thickness was 1 mm for Au and 5 mm for Al and Nb. For Ni, both of 2.5 and 5.0 mm thick pellets were used. These pellets were packed in the Aluminum capsules having outer diameter of 9.4 mm with thickness of 0.5 mm, and then were inserted in the irradiation holes. W and Pb pellets were also filled in the capsules to prevent the perturbation of neutron flux. The surface of the irradiation hole was covered with 1.3 mm thick SS plate.

The number of incident protons were measured with a calibrated pick up coil (7) installed in the beam line and a Faraday cup using the lead assembly itself. The number of incident protons were estimated with accuracy of 3%. The shape of the beam was about 2.5 and 1.5 cm in FWHM in the horizontal and vertical directions, respectively.

The γ-ray spectrum of irradiated pellets were measured repeatedly from one day after irradiation to a few months. The peak efficiency of Ge-detector was determined using standard radionuclide sources with accuracies ranged from 1.5 to 2.0%. The errors of the efficiency was estimated as 5% through this calibration. The reaction rate of each activation detector was obtained from the peak counts of γ-ray spectrum by correcting the decay, peak efficiency, self absorption of γ-rays in a pellet and the coincidence sum effect in counting.

3. Calculation

The tungsten/lead assembly was modelled in a two-dimensional cylinder as shown in Fig. 2. The SS liner in the assembly was also taken into account in the two-dimensional geometry model. The reaction rates were obtained in the cells with 2 cm width along the longitudinal direction.

The neutron flux in the tungsten/lead assembly was calculated with NMTC/JAERI in combination with MCNP4A. NMTC/JAERI simulates the nuclear reactions and particle transport in the energy region above 20 MeV by the use of the intranuclear cascade model of Bertini (8) and a particle evaporation model taking account of the high energy fission process. The level density parameter derived by a formulae of Ignatyuk (9) was used in the evaporation calculation. The cut-off energies for particle transport were set to be 20 MeV for neutron and 2 MeV for charged particles. The energy group structure defined in the HILO-86R library (10) was employed up to 400 MeV in this calculation. For neutrons above 400 MeV, the energy group structure was extended with an interval of 50 MeV. The reaction rate was obtained with the nuclide production cross sections calculated by the ALICE-F code (11). Here, some of calculated cross sections were adjusted to connect smoothly with the ones compiled in JENDL Dosimetry file (12) at 20 MeV. These cross sections are shown in Fig. 3.

MCNP4A calculates the transport of the neutrons in the energy region lower than 20 MeV using a continuous energy cross section library which has been processed from JENDL-Fusion File (13). Transport of charged particles with energies below 2 MeV was not treated in this calculation.

The histories of 2 millions of incident protons were calculated with the conditions that the incident beam shape was expressed by the Gaussian distribution with FWHMs of 2.5 and 1.5 cm in horizontal and vertical direction. The importance sampling technique was employed to obtain an enough statistics for estimating the neutron flux.

4. Results and Discussion

Figure 4 shows the reaction rate distribution of the $^{27}Al(n,x)^{24}Na$ reaction measured in the tungsten/lead assembly bombarded with 500 MeV protons. For comparison, the results of the previous experiment (5) are shown with the open marks in the Figure. It is observed that the reaction rate shows the maximum value around 25 cm from the front surface of the lead assembly and decreases with the distance. The width of longitudinal reaction rate distribution in tungsten target is narrower than that in lead one. This characteristics is attributed to the following physical aspects: The range of 500 MeV proton is about 12 cm for tungsten, while 20 cm for lead. The mean free path of fast neutron is shorter in tungsten than in lead because of large macroscopic total cross section of tungsten.

Figure 5 shows the measured and calculated reaction rates of the $^{nat}Ni(n,x)^{58}Co$ reaction in the tungsten/lead assembly. The calculation reproduces the shape of the measured reaction rate distribution well. Quantitatively, however, the calculation overestimates the measured reaction rates at the whole positions. The $^{nat}Ni(n,x)^{58}Co$ reaction is induced predominantly by the neutrons in the MeV region. Moreover, the cross section of this reaction is evaluated very well. Thus, this discrepancy indicates that the NMTC/JAERI-MCNP4A code system overestimates the neutron yield in the MeV region. This overestimation is attributable to the lack of the preequilibrium process in the nuclear reaction calculation in NMTC/JAERI. The excitation energy of a residual nucleus in the evaporation process is estimated somewhat higher so that the number of MeV neutrons emitted from the nucleus might be overestimated.

Figure 6 shows the measured and calculated reaction rates of the $^{197}Au(n,2n)^{196}Au$ reaction in the tungsten/lead assembly. The calculation is in good agreement with the experiments although slight discrepancies are observed at the longitudinal positions of 5, 55 and 65 cm from the front surface. The $^{197}Au(n,2n)^{196}Au$ reaction is sensitive to the neutrons from 10 to 20 MeV. As shown in Figs 7 and 8, good agreement is observed between the calculations and the experiments for the $^{27}Al(n,x)^{24}Na$ and $^{93}Nb(n,2n)^{92m}Nb$ reactions sensitive to the neutrons from 10 to 20 MeV, respectively. Consequently, it can be concluded that the NMTC/JAERI-MCNP4A code system estimates well the neutron yield in the energy region of 10 to 20 MeV for tungsten target.

Figures 9 and 10 show the reaction rate distributions of the $^{197}Au(n,4n)^{194}Au$ and $^{93}Nb(n,4n)^{90}Nb$ reactions in the tungsten/lead assembly, respectively. These reactions are sensitive to the neutrons in the energy region of 30 to 45 MeV where the production and transport of neutrons is treated by the NMTC/JAERI code. It is observed in Fig. 9 that the NMTC/JAERI calculation underestimates the measured reaction rates by 20 to 30% for the $^{197}Au(n,4n)^{194}Au$ reaction at almost all the positions. This result is similar with that of the previous experiment (5) using the pure lead assembly. On the other hand, good agreement is observed between the calculation and the experiment for the $^{93}Nb(n,4n)^{90}Nb$ reaction sensitive to neutrons with 30 to 40 MeV.

In Fig. 11, the total and the elastic neutron cross sections (14) for tungsten used in NMTC/JAERI are compared with those in an evaluated nuclear data file of Los Alamos National Laboratory (15). Not only the total cross section but also the fraction of non-elastic one used in NMTC/JAERI is higher than the evaluated data. This suggests that the mean free path of neutrons in the energy region below 30 MeV might be estimated short in the NMTC

/JAERI calculation. However, this can be not confirmed in this integral experiment because of lack of available neutron spectrum data for thick tungsten target. It is noted that the nuclide production cross sections calculated by the ALICE-F code have not been evaluated yet. This is the other source of the discrepancy observed in the reactions sensitive to this energy range.

5. Conclusions

Reaction rate distributions of various activation detectors sensitive to 1 to 30 MeV were measured in the volume of 60 cm in diameter and 100 cm in length of the tungsten/lead assembly with 500 MeV proton bombardment. The reaction rate distributions were analyzed with the NMTC/JAERI-MCNP4A code system using the nuclide production cross section values combining JENDL Dosimetry File and the ALICE-F calculation.

It was found that the code system gave higher reaction rates than the experiment for the activation detector sensitive to the MeV region. Good agreement was obtained between the calculation and the experiment for the activation detectors sensitive to neutrons in the energy region from 10 to 20 MeV. For the activation detectors with threshold energies above 20 MeV, agreement between the calculations and the experiments was different among reactions because of ambiguity of reaction cross sections. Nevertheless, the calculation using the NMTC/JAERI-MCNP4A code system reproduced the measured reaction rate distributions with an accuracy of 20 to 30 %.

Acknowledgements

This experimental work was carried out under the contract on the facility utilizations of KEK. The authors would like to thank the staffs of neutron science laboratory for operation of booster synchrotron and are also indebted to those of radiation science center of KEK for kind instruction to treatment of irradiated samples.

References

(1) Y.Nakahara, T.Tsutsui: "NMTC/JAERI A Code System for High Energy Nuclear Reactions and Nucleon-Meson Transport Code", JAERI-M 82-198 (1982), [in Japanese].; H.Takada, et al.:"Au Upgraded Version of the Nucleon Meson Transport Code : NMTC/JAERI97", JAERI-Data/code 98-005 (1998).

(2) J.F.Briesmeister (Ed.) : "MCNP A General Monte Carlo N-Particle Transport Code, Version 4A", LA-12625, (1993).

(3) T.Mukaiyama, Y.Oyama, M.Mizumoto, T.Takizuka, R.Hino, : "Neutron Science Project at JAERI", Proc. of the Topical Mtg. on Nucl. Applications of Accel. Technol., Albuquerque, New Mexico, Nov. 16-20, 1997. pp. 398-404, (1997).

(4) S.Meigo, et al.: "Measurements of Spallation Neutrons from a Thick Lead Target Bombarded with 0.5 and 1.5 GeV Protons", Joint Proc. of the 13th Mtg. of the Int. Collaboration on Advanced Neutron Sources held at Paul Scherrer Institute, Oct. 11-14, 1995 and 4th Plenary Mtg. of the European Spallation Source Project, ESS, held at Weinfelden, Oct. 16-19, 1995, PSI-Proceedings 95-02, pp.442-453, (1995).

(5) H.Takada, et al.: "Measurement of Reaction Rate Distributions in A Lead Assembly Bombarded with 500 MeV Protons", Proc. of the 3rd Workshop on Simulating Accel. Radiat. Environments (SARE3), May 7-9, 1997, KEK, tsukuba, Japan, KEK Proceedings, 97-5, 284 (1997).

(6) T.Nakamoto, et al.: J. Nucl. Sci. Technol. **32** (1995) 827.; K.Ishibashi, et al.: J. Nucl. Sci. Technol. **34** (1997) 529

(7) Y.Irie, Y.Yano: Nucl. Instrm. Method Phys. Res. A **320**, (1992) 27.

(8) H.W.Bertini : Phys. Rev. **188**, (1969) 1711 .
(9) A.V.Ignatyuk, G.N.Smirenkin, A.S.Tishin : Sov. J. Nucl. Phys. **21**, (1975) 256 .
(10) H.Kotegawa, Y.Nakane, A.Hasegawa, Sh.Tanaka :"Neutron-photon Multigroup Cross Sections for Neutron Energies up to 400 MeV; HILO86R", JAERI-M 93-020, (1993).
(11) T.Fukahori :"ALICE-F Calculation of Nuclear Data up to 1 GeV", Proc. of the Specialists' Mtg. on High Energy Nucl. Data, Oct. 3-4, 1991, JAERI, Tokai, JAERI-M 92-039, pp. 114-122 (1992).
(12) M.Nakazawa, et al. : "JENDL Dosimetry File", JAERI-1325, (1992).
(13) S.Chiba, B.Yu, T.Fukahori : "Evaluation of JENDL Fusion File", Proc. of the 1991 Symp. on Nucl. Data, Nov. 28-29, 1991, JAERI, Tokai, Japan, JAERI-M 92-027, pp. 35-44 (1992).
(14) S.Pearlstein : Astrophys. J. **346**, (1989) 1049.
(15) M.B.Chadwick, et al.:"Cross Section Evaluations to 150 MeV for Accelerator-Driven Systems and Implementation in MCNPX", LA-UR-98-1825 (1998).

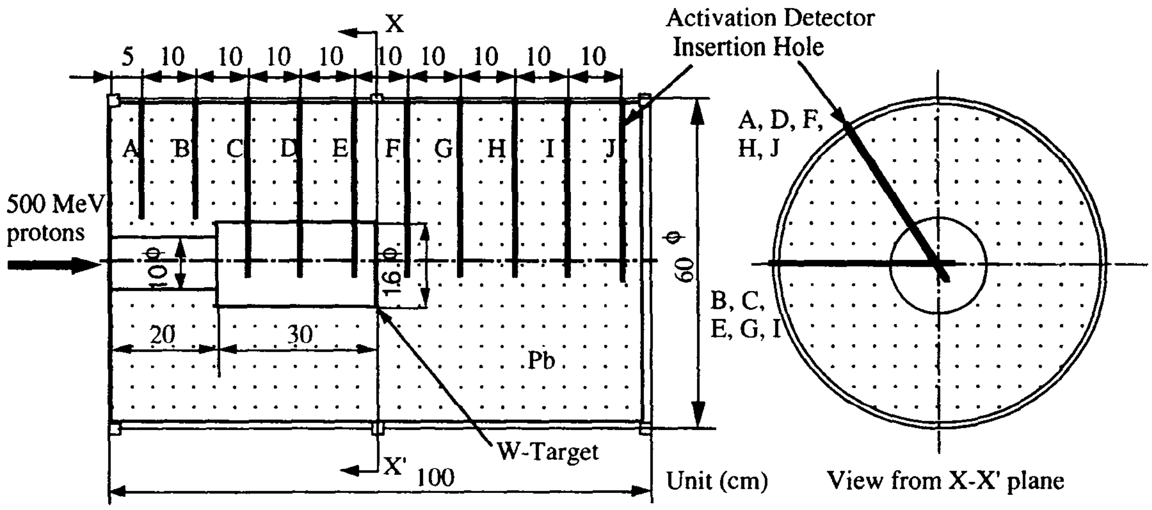

Fig. 1 Cross sectional view of the tungsten/lead assembly. The characters A to J indicate the irradiation hole for activation detectors.

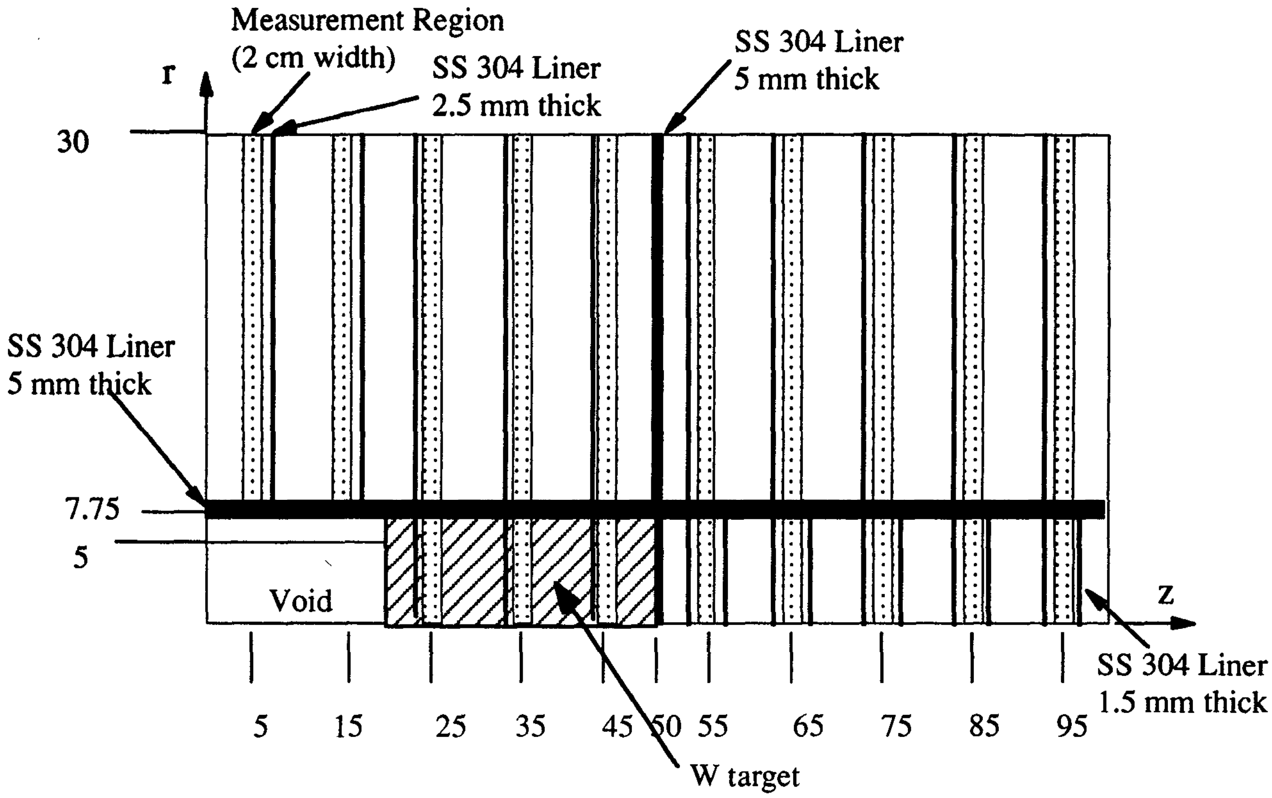

Fig. 2 Illustraion of the geometry model of the tungsten/lead assembly for analysis using the NMTC/MCNP4A code system.

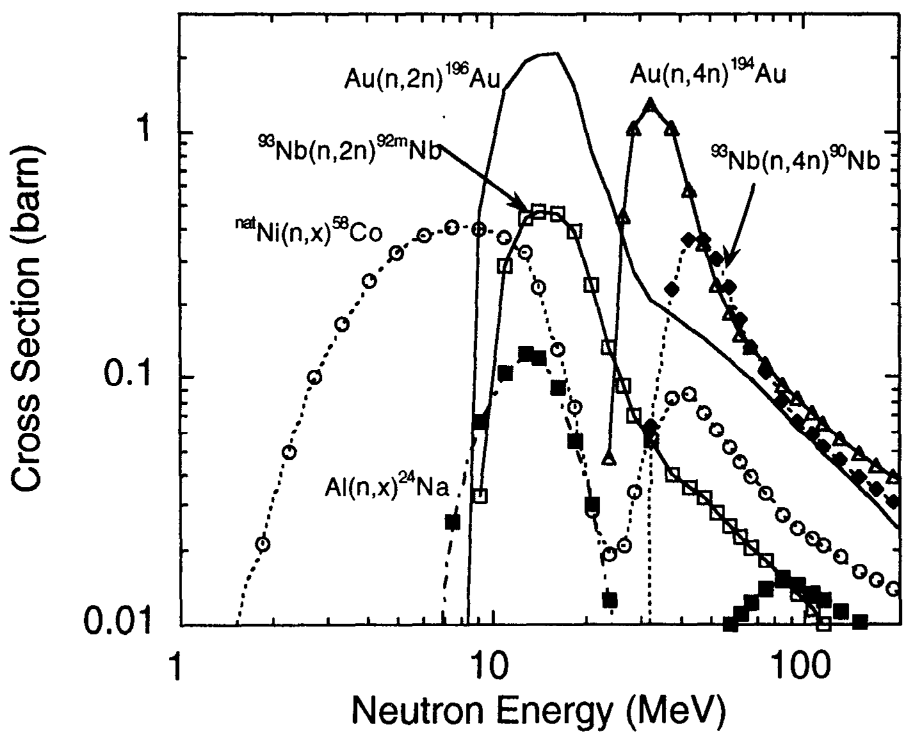

Fig. 3 Neutron cross sections of the reactions of $^{nat}Ni(n,x)^{58}Co$, $^{27}Al(n,x)^{24}Na$, $^{198}Au(n,2n)^{196}Au$, $^{93t}Nb(n,2n)^{92m}Nb$, $^{93t}Nb(n,4n)^{90}Nb$ and $^{198}Au(n,4n)^{194}Au$ employed in the calculation of reaction rate. The data below 20 MeV are taken from JENDL Dosimetry file (12). Those above 20 MeV are calculated by ALICE-F (11).

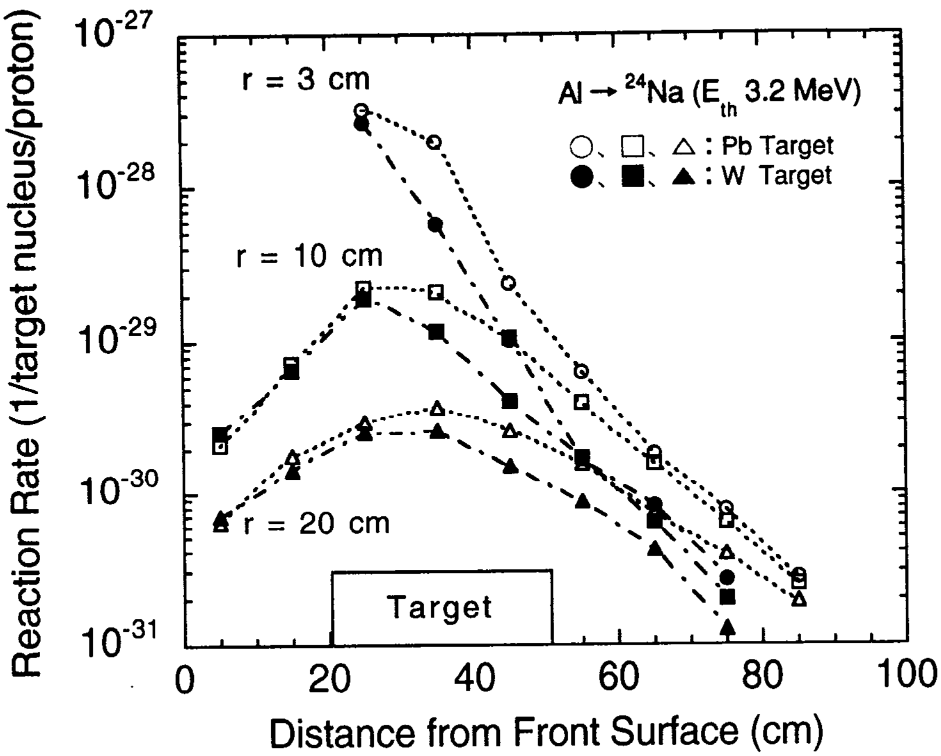

Fig. 4 Measured reaction rate distributions of the $^{27}Al(n,x)^{24}Na$ reaction in the lead assemblies bombarded with 500 MeV protons. The open and solid marks indicated the measured data for lead/lead assembly [(5)] and for tungsten/lead one, respectively.

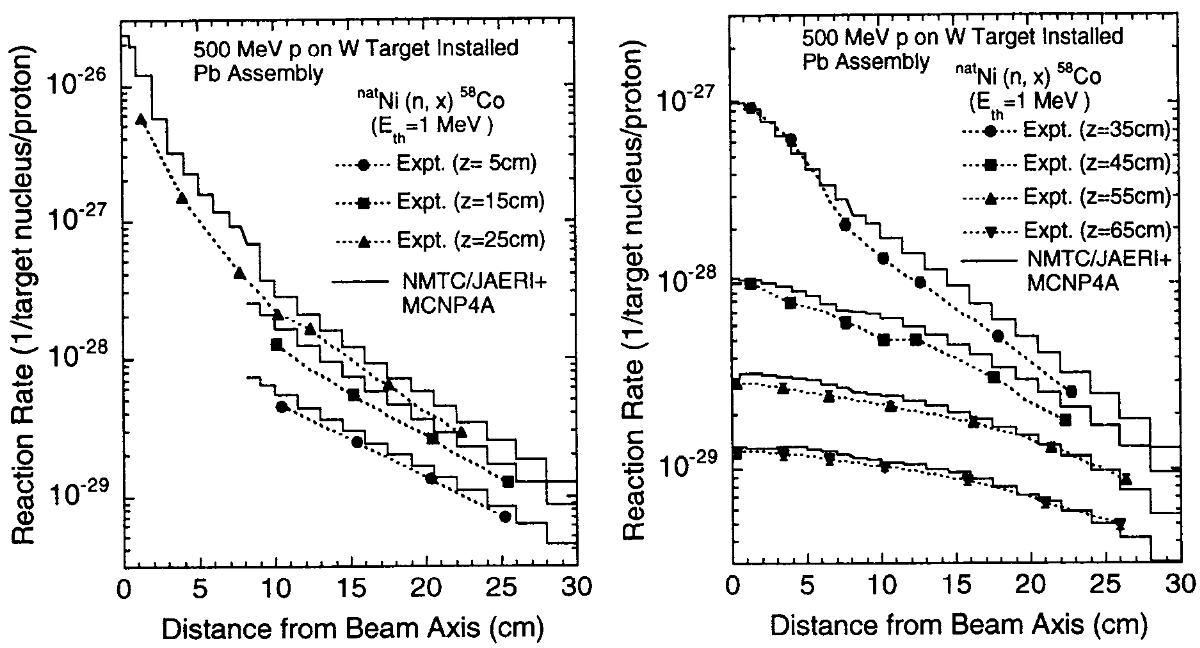

Fig. 5 Reaction rate distribution of the $^{nat}Ni(n,x)^{58}Co$ reaction in the tungsten/lead assembly bombarded with 500 MeV protons. The solid marks and lines indicate the experimental results and the calculation using the NMTC/JAERI-MCNP4A code system, respectively. The dotted lines are for eye guide. The character 'z' means the depth of the assembly where activation detectors were inserted.

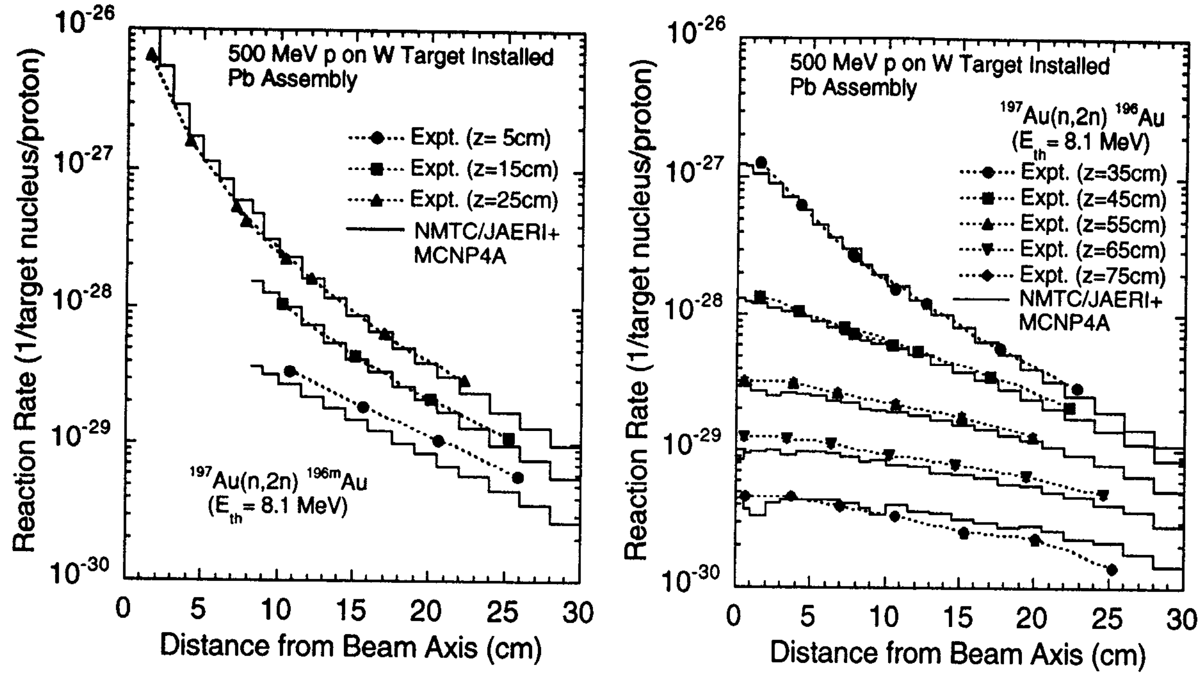

Fig. 6 Reaction rate distribution of the ^{197}Au(n,2n)^{196}Au reaction in the tungsten/lead assembly bombarded with 500 MeV protons. The notes to the marks and lines are the same as for Fig. 5.

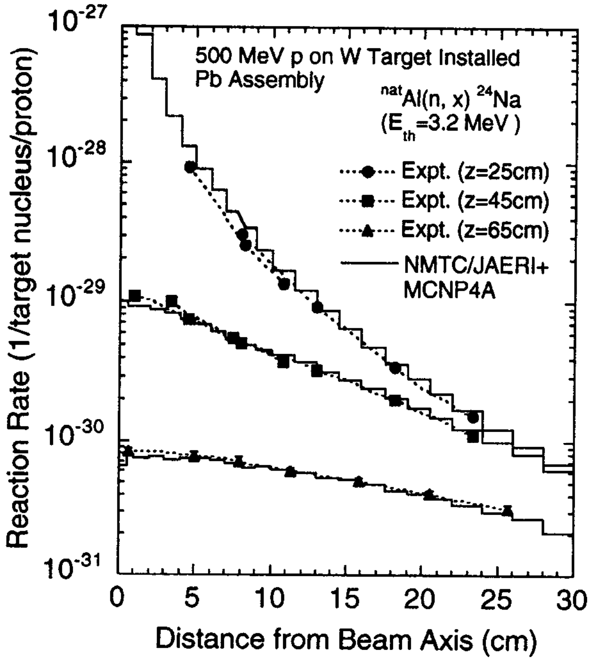

Fig. 7 Reaction rate distribution of the ^{27}Al(n,x)^{24}Na reaction in the tungsten/lead assembly bombarded with 500 MeV protons. The notes to the marks and the lines are the same as for Fig. 5.

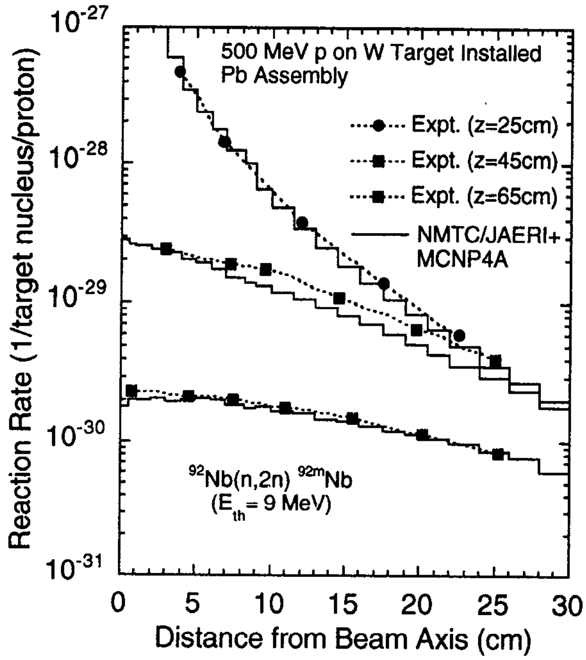

Fig. 8 Reaction rate distribution of the ^{93}Nb(n,2n)^{92m}Nb reaction in the tungsten/lead assembly bombarded with 500 MeV protons. The notes to the marks and the lines are the same as for Fig. 5.

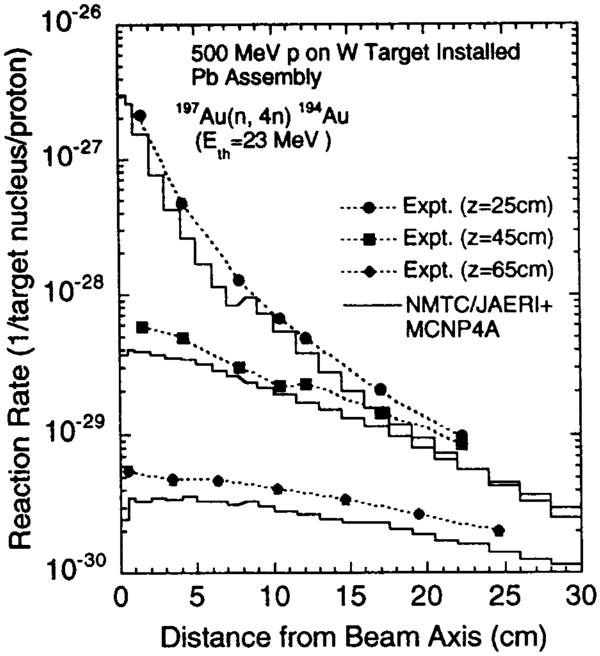

Fig. 9 Reaction rate distribution of the $^{197}Au(n,4n)^{194}Au$ reaction in the tungsten/lead assembly bombarded with 500 MeV protons. The notes to the marks and the lines are the same as for Fig. 5.

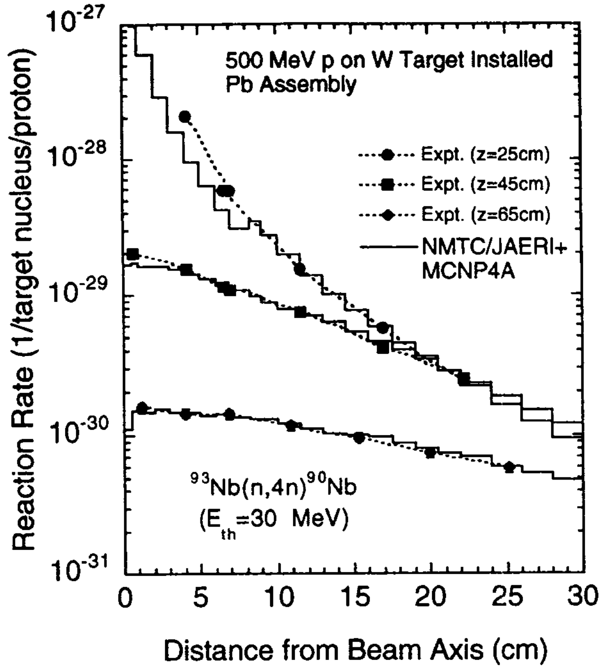

Fig. 10 Reaction rate distribution of the $^{93}Nb(n,4n)^{90}Nb$ reaction in the tungsten/lead assembly bombarded with 500 MeV protons. The notes to the marks and the lines are the same as for Fig. 5.

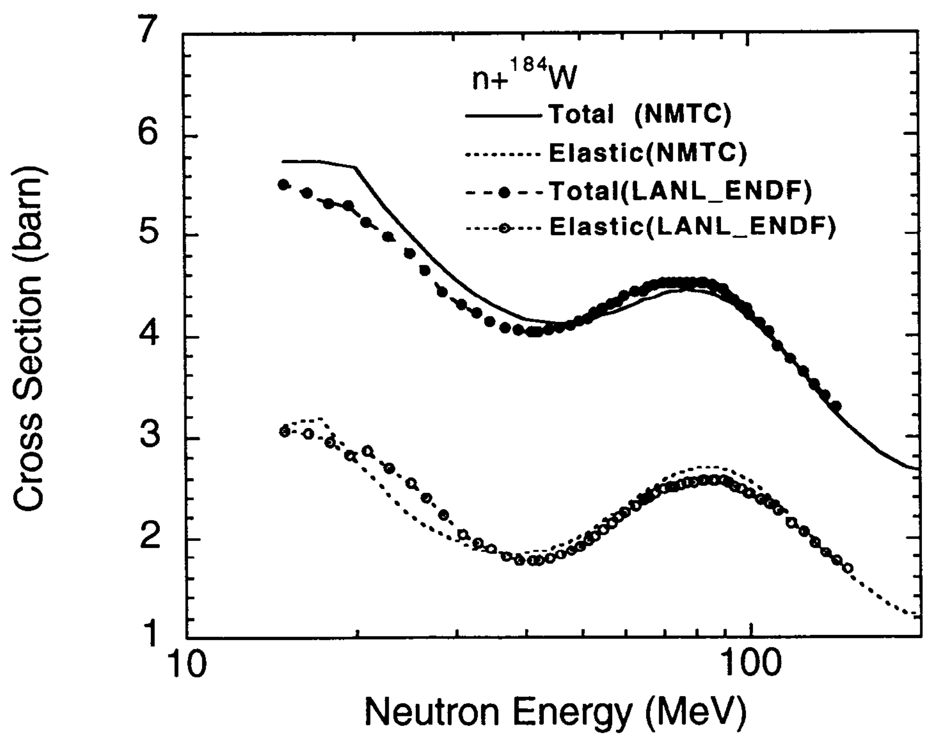

Fig. 11 Comaprison of neutron cross sections of ^{184}W. The solid and dotted lines indicate the total and elastic cross sections [14] emoployed in NMTC/JAERI. Those with marks stand for the cross sections evaluated by Chadwick et al. [15].